

COVER SHEET

Title: Experimental verification of the eddy-current inerter system with cable bracing
for seismic mitigation

Authors: Songtao Xue
Xinlei Ban
Liyu Xie

ABSTRACT

In this study, a novel vibration mitigation device which uses a displacement amplification mechanism is proposed. It is called cable-bracing inerter system (CBIS) and provides the additional damping force through inerter element, friction element and eddy current damping element. Eddy current damping is a non-contacting damping mechanism, and the damping ratio can be easily adjusted by varying the air gap between the permanent magnets and the conductor in this device. In the traditional tuned mass dampers, large additional mass is often required for its seismic control which is a limitation of a tuned mass damper. This device overcomes this kind of limitation and its effective masses can be several times than the actual mass. In this paper, we present a comprehensive study that involves experimental, analytical, and computational approaches. First, we described the principle of the CBIS which includes eddy current damping mechanism and an apparent mass amplifier using inerter. CBIS utilizes two cables which are easy to install to transmit control forces and deformation between the main structure and CBIS. Second, the theoretical model was given and to simplify the theoretical model of CBIS, the flexibility of the cable was neglected and the motion governing equation was also given. A series of free vibration tests and shaking table tests were conducted on a single degree of freedom (SDOF) steel-frame model with/without a CBIS to evaluate the effectiveness and performance of the CBIS in suppressing the vibration of the model. In the free vibration tests, the extend Kalman filter is used to identify the parameters of structure and CBIS. The results show that by using a properly designed inerter system, a lightly damped primary system can achieve a considerable reduction in its response with a small weight penalty. The experimental results show that the CBIS can effectively reduce the displacement and acceleration responses under different earthquake excitations.

INTRODUCTION

The traditional damping device is mainly composed of three classical mechanical components, namely mass, spring and damper. The inerter, proposed by Smith [1] in the early 2000s, is a two terminals device with the property that the force through the terminals is proportional to the relative acceleration between them:

$$p = m_d (a_2 - a_1) \quad (1)$$

where p is the axial resistive force of the inerter; m_d is the inertance; a_1 , a_2 are respectively the accelerations at the two terminals of the inerter. With the gearing included in the device, the inerter can have a far higher inertance than its physical mass. The principal advantage of the inerter is that a high level of vibration isolation can be achieved with low amounts of added mass.

Recently, a tuned viscous mass damper (TVMD), which mainly consists of viscous damping system and rotational inertial mass, is proposed by Saito et al.[2]. Ikago et al.[3, 4] proposed the TVMD design methods for SDOF and multiple-degree-of freedom structures. In 2013, Lazar et al.[5] proposed a tuned inerter damper (TID) configuring an inerter arranged in series with spring and damper elements and compared its performance with that of a traditional TMD. Pan et al.[6, 7]. suggested that the design of SDOF system with TVMD should be based on structural performance requirements. Kim et al.[8] proposed a rotational friction damper connected to tension-only braces to dissipate seismic-induced energies. Kurata et al. [9] developed a seismic retrofit technique by combining cable braces and energy dissipater. Because the costs of cables are much lower than the mechanical devices such as gears or ball-screw mechanisms and the use of cables in developing energy dissipater is yet to be investigated, looking for another alternative with cable bracing is possible and necessary.

In this paper, an innovative CBIS which uses a displacement amplification mechanism will be proposed. The next sections of this paper will introduce the mechanical mode and the operating principle of CBIS, followed by the study of inherent vibration characteristics of an SDOF structure with the inerter system. To verify the effectiveness of CBIS, an SDOF steel frame is specifically designed and subjected to free and forced vibration tests with and without the presence of CBIS.

THEORETICAL ANALYSIS OF CBIS

Mechanical model of CBIS

CBIS is an inerter-system using eddy currents. Eddy current damping is a non-contacting damping mechanism. It's damping ratio can be easily adjusted by changing the air gap between the permanent magnets and the conductor. We invented the rotational eddy currents working mode (shown in Figure 1), and the 12 magnets are on the same side. It is easy to change the distance between the copper plate and the magnet to adjust the damping coefficient because there are several holes for fixing the positions of copper plates at regular intervals on the roller. A CBIS consists of a rotor and a stator. The rotor is made up of two conductor plates (diameter 190mm) and a roller (diameter 25mm). The stator includes two side plates fixed to the base with width \times length \times height dimensions of 240mm \times 200mm \times 12mm, two bearings for supporting the roller, and 24

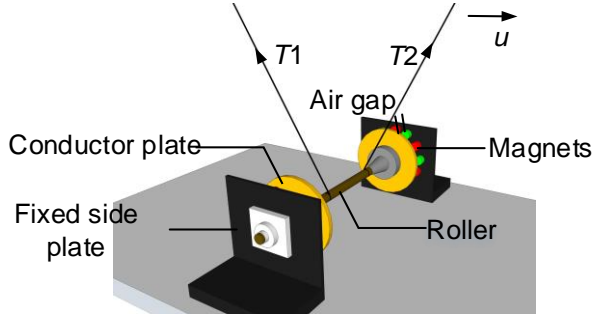


Figure 1. Component elements of novel CBIS.

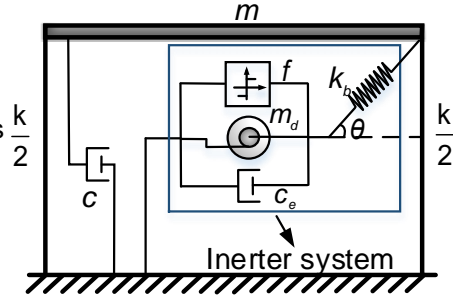


Figure 2. Analytical model

permanent magnets adsorbed on two side plates equally. The conductor plate is made of copper plate whose electrical conductivity is high, and the magnetic field source is selected from Neodymium (NdFeB) cylindrical permanent magnets (diameter 25mm, thickness 20mm), and the magnetic poles are staggered according to the principle of opposite magnetic poles of adjacent magnets.

Only tensile forces are induced in the two cables. The mechanical system of CBIS consists of eddy current damping element, inerter element, friction element and the spring element. The damping element is set in parallel with the inerter element and the friction element to form a component and the spring element is then connected with the component in series. Figure 2 shows the mechanical mode of an SDOF structure equipped with CBIS and its layout relationship in the horizontal direction. m , c , and k are the mass, damping coefficient, and stiffness of the SDOF system, the primary structure, respectively; f stands for the friction and can be calculated by $f = f_0 \text{sgn}(\dot{\phi})$; m_d is the inertance of the CBIS. J is the mass moment of inertia of the inerter and r_0 is the radius of the roller. The small actual mass can be amplified to large apparent mass by attaching the inerter element. $c_e = c_d \cos^2 \theta$ is the equivalent damping coefficient in horizontal direction of the CBIS and k_b is the stiffness of the spring element. The output force of this inerter system is the resultant force of the inerter element, friction element and the eddy current damping element.

Motion governing equation

According to the analytical model shown in Figure 2, the equations of motion for this SDOF structure with a CBIS under external excitations can be written as follows:

$$\begin{cases} m\ddot{u}(t) + c\dot{u}(t) + ku(t) + k_b(u(t) \cos \theta - \phi(t)r_0) \cos \theta = -ma_g(t) \\ J\ddot{\phi}(t) + c_d\dot{\phi}(t)r_0^2 + fr_0 = k_b(u(t) \cos \theta - \phi(t)r_0)r_0 \end{cases} \quad (2)$$

This means that the ground motion acceleration is transmitted through the inerter element. In fact, the steel cable has a very large stiffness. To simplify the analytical model of CBIS, the flexibility of the cable is neglected, and the motion equation is:

$$\left(m + \frac{J \cos^2 \theta}{r_0^2} \right) \ddot{u}(t) + (c_0 + c_d \cos^2 \theta) \dot{u}(t) + ku(t) + f \cos \theta = -ma_g(t) \quad (3)$$

In Equation (3), $J \cos^2 \theta / r_0^2$ is the inertance of the inerter element.

EXPERIMENTAL DESIGN AND PROCEDURE

The experimental work included free and shaking table tests. These tests were applied to the structure with CBIS system as well as the bare structure. Natural frequencies and the damping ratio of the bare structure were obtained from free vibration tests. Forced vibration tests were used to determine the dynamic responses of the bare structure. The dynamic responses of the structure with systems under a wide range of excitation frequencies were also determined through forced vibration tests.

To examine the performance of the proposed device, CBIS is incorporated into an SDOF system. The experimental model consists of a single-story steel frame and a CBIS, and Figure 3 shows the configuration of the model. The specification of the test frame is listed in Table 1. The frame columns consist of steel plates (yield strength: 235MPa) with width \times length \times height dimensions of $5 \times 60 \times 1000$ mm. The slabs consist of steel plates (yield strength: 235MPa) with plane dimensions of 834×390 mm and a thickness of 10mm. To measure structural responses, three types of sensors are installed. The acceleration of the floor is measured by accelerometers, A1. The displacement of the top floor and the platform of a shake table is measured by two displacement meters D1 and D2. In addition, two force sensors are stalled in the steel cables to measure the tension of steel cables.

Three types ground motions El Centro wave (1940, NS), Japan 311 wave (2011, NS), and Shanghai artificial wave (SHW2, 1996) are utilized in the shaking table tests to investigate the vibration control effects of CBIS under different seismic actions. Each type of seismic wave acts along only one direction, and the peak value of the acceleration increases gradually from 0.1g to 0.3g with the interval of 0.1g (g is the acceleration due to gravity) which are chosen to represent moderate, severe and maximum probable earthquakes.

FREE VIBRATION TESTS

In order to calculate natural frequencies and the damping ratio of the test frame, a

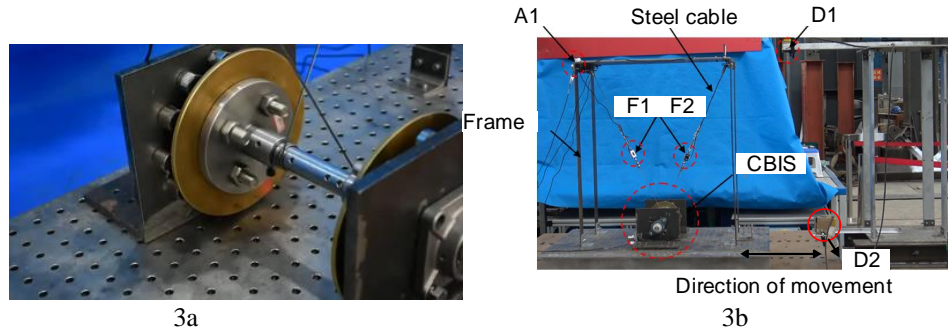


Figure 3. Photograph of the experimental specimens

series of free vibration tests was carried out first. The top of the test structure was pulled for around 80 mm and then it was released to vibrate freely. The time histories of displacement and acceleration responses of the frame were measured for 15 seconds. In order to extract the natural frequencies of the test structure, the acceleration responses were decomposed by the Fast Fourier Transform (FFT). Figure 4 displays the FFT results obtained from the recorded time history of acceleration, and the natural frequency of the test frame is 0.915Hz, which represents typical structures in civil engineering.

Then, the extend Kalman filter (EKF) is adopted to identify primary structure parameters: stiffness and damping coefficient. Limited by space, the detailed calculating process of EFK will not be described in this paper. The identification results are listed in Table I.

TABLE I. SPECIFICATIONS FOR THE PRIMARY SYSTEM

Mass m (kg)	Stiffness k (N/m)	Primary damping ratio %	Frequency (Hz)
23	762.23	0.36	0.917

The additional damping force generated by CBIS includes two mainly parts (the effect of friction is ignored in this paper): eddy current damping element and inerter element. These two parts can be divided easily by adding the magnets or not. In the tests, first, the frame equipped with the inerter element not adding magnets, in other words, only installing inerter element, was pulled for 80mm and then it was released to vibrate freely. And then the frame equipped with the inerter element and the eddy current damping element was pulled again to evaluate the effectiveness of the CBIS.

The effect of the inerter element is related to the inertia of the inerter, namely the thickness of the conductor plates. In the free vibration tests, the conductor plates of three thicknesses are used, 5mm,10mm. Figure 5a and 5b compares different displacement and acceleration responses of an SDOF steel frame with different inerter elements. After adding the eddy current damping element, the displacement and acceleration responses are shown in Figure 5c and 5d. For the convenience of recording and processing the test data, the conditions naming principle is: Conductor plate quality + thickness(mm)-the inerter element (I)/the eddy current damping element (E)-air gap size(mm).

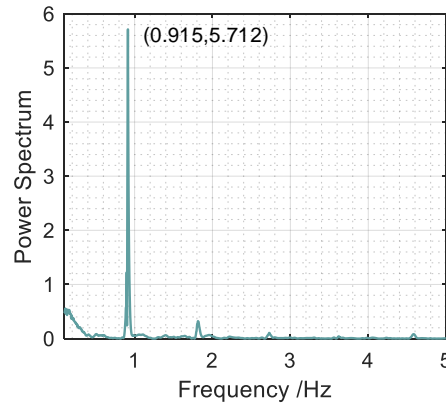


Figure 4. FFT result for the recorded time history of acceleration on the top of the structure

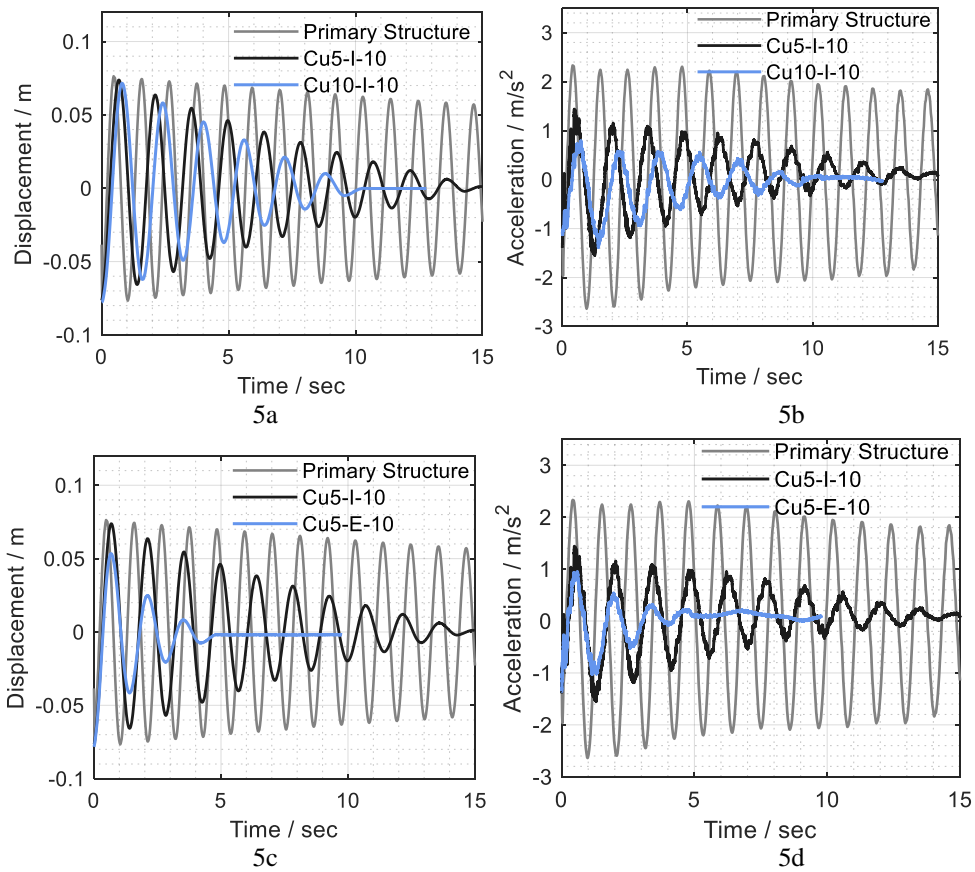


Figure 5. Displacement and acceleration responses of the test frame

Using the EKF to identify the parameters of structure with CBIS: stiffness and damping coefficient, the results are listed in TABLE II. When an inerter element is installed on the test structure, its mass is added to the total mass of the bare structure. This alters the natural frequency of the test structure (from 0.915Hz to 0.721Hz, 0.665Hz).

TABLE II. SPECIFICATIONS FOR THE CONTROLLED SYSTEM

Test conditions	Inertance (kg)	Identification Frequency (Hz)	Test Frequency (Hz)	Error %	Damping ratio %	Friction (N)
Cu5-I-10	12.03	0.743	0.721	3.05	-	7.540
Cu10-I-10	23.95	0.642	0.665	3.46	-	15.509
Cu5-E-10	12.03	0.743	0.721	3.05	8.56	9.807

The inerter is used to absorb vibrational energies and then friction element and damping element will dissipate these energies. In Figure 5a and 5b, energy is absorbed by different inerter elements, and dissipated by friction element, when the magnets are not installed in the device. Friction is mainly produced at the connection between the roller and the bearing, which is proportional to the pressure. When the thickness of the conductor changes from 5mm to 10mm, increased pressure causes friction to increase from 7.540N to 15.509N. It can also be seen that, compared to the test frame, the decay both in the displacement and in the acceleration responses of frame with the inerter element is much faster, especially after the eddy current damping element is installed

on the device. In this case, the air gap is 10mm, and the damping ratio is 8.56%. A comparison between Figure 5c and 5d shows that the decay in the displacement and acceleration responses of the bare test structure is faster than the case in which only inerter element is employed (Figure 5a and 5b).

SHAKING TABLE TESTS

The time histories of the displacement and acceleration responses at the roof of the test frame with 5 mm copper plates as the conductor plate under the El Centro (0.1g) are shown in Figure 6a and 6b. The responses of the test frame under other seismic waves will not be described in this paper limited by space. The CBIS significantly reduced the responses over the entire period.

The peak value and the root-mean-square (RMS) value of the displacement and acceleration responses are chosen to evaluate the damping performance of CBIS. These two values are important controlling indices in structural vibration control. The peak value reflects the dynamic response at a certain instant, whereas the RMS value relates to the vibration energy and reflects the responses over an entire period. The vibration reduction effect is defined as follows:

$$\text{Reduction effect} = \frac{\text{Response without CBIS} - \text{Response with CBIS}}{\text{Response without CBIS}} \quad (4)$$

Tables III list the displacement and acceleration responses at the roof of the test frame with 5 mm copper plates as the conductor plate under different seismic wave intensities, respectively, including the peak value and the RMS value.

TABLE III. ACCELERATION RESPONSE REDUCTION EFFECT

Seismic input	El Centro		Japan 311		SHW2	
	Peak	RMS	Peak	RMS	Peak	RMS
0.1g	72.88	88.46	48.78	75.00	74.00	89.47
0.2g	70.19	87.76	45.12	72.00	67.39	85.29
0.3g	76.80	89.16	45.08	70.00	60.71	80.00

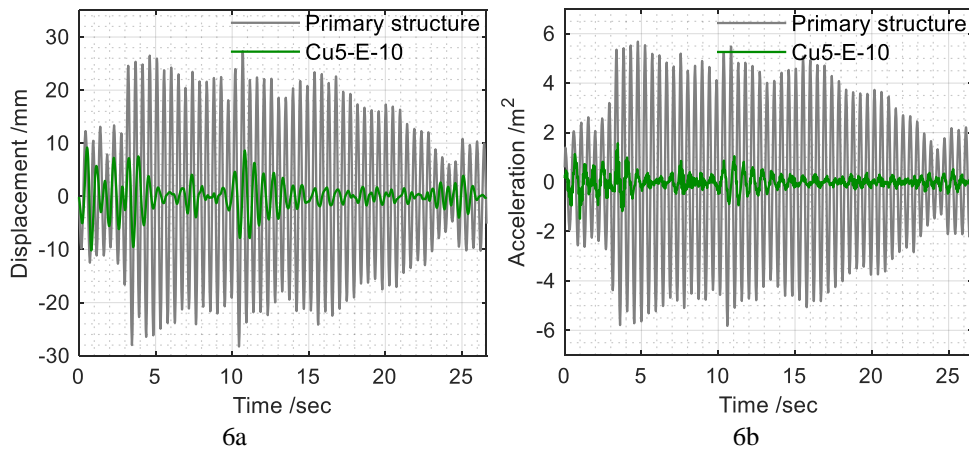


Figure 6. Response time histories at the roof of the test frame: (a) Displacement, El Centro (0.1g); (b) Acceleration, El Centro (0.1g)

The best vibration control effects for the peak and RMS values of the acceleration responses were 76.80% and 89.47% (marked in bold). The responses of the test frame with CBIS attached were smaller than those of the uncontrolled structure, which demonstrates the efficient attenuation effects from CBIS. In addition, the vibration control effects for the RMS response were generally more obvious than those for the peak response, which indicates that CBIS efficiently attenuated the entire response of the primary structure over a period of time.

CONCLUSION

An energy dissipater that uses new transmission system was proposed in this paper. A series of free vibrations and shaking table tests were conducted to investigate the inerter system's performance. The results show that the structural displacement and acceleration responses can be reduced significantly with the help of a CBIS. The displacement control effects of the frame installing the CBIS with 10mm conductor plates is better than that with 5 mm conductor plates. The maximum and RMS responses of the SDOF structure were reduced by attaching the new inerter system under both onsite earthquake excitations and artificial waves. Additionally, the CBIS still exhibited certain vibration control effects when the seismic input was maximum probable earthquakes 0.3g, which suggested the robustness of the CBIS.

REFERENCES

1. Smith, M.C. 2002. "Synthesis of mechanical networks: the inerter," *IEEE Transactions on Automatic Control*, 47(10): 1648-1662.
2. Kenji Saito, Shigeki Nakaminami, Hidenori Kida, and Norio Inoue. 2008. "Vibration tests of 1-story response control system using inertial mass and optimized softy spring and viscous element." *14th World Conference on Earthquake Engineering*, pp. 12-01.
3. Ikago, K., K. Saito, and N. Inoue. 2012. "Seismic control of single-degree-of-freedom structure using tuned viscous mass damper," *Earthquake Engineering & Structural Dynamics*, 41(3): 453-474.
4. Ikago, K., et al. 2012. "Modal Response Characteristics of a Multiple-Degree-Of-Freedom Structure Incorporated with Tuned Viscous Mass Dampers," *Journal of Asian Architecture & Building Engineering*, 11(2): 375-382.
5. Lazar, I.F., S.A. Neild, and D.J. Wagg. 2014. "Using an inerter-based device for structural vibration suppression". *Earthquake Engineering & Structural Dynamics*, 43(8):1129-1147.
6. Pan, C. et al. 2017. "Demand-based optimal design of oscillator with parallel-layout viscous inerter damper," *Structural Control & Health Monitoring*, 25(9):e2051.
7. Pan, C. and R. Zhang. 2018. "Design of structure with inerter system based on stochastic response mitigation ratio," *Structural Control & Health Monitoring*, 25(6):e2169.
8. Kim, J.H. Choi, and K.W. Min. 2011. "Use of rotational friction dampers to enhance seismic and progressive collapse resisting capacity of structures," *Structural Design of Tall & Special Buildings*, 20(4):515-537.
9. Kurata, M. R.T. Leon, and R. Desroches. 2012. "Rapid Seismic Rehabilitation Strategy: Concept and Testing of Cable Bracing with Couples Resisting Damper," *Journal of Structural Engineering*, 138(3):354-362.



DEStech Publications, Inc.

CONTRIBUTING AUTHOR COPYRIGHT RELEASE FORM

As author of the chapter/contribution titled Experimental verification of the eddy-current inerter system with cable bracing for seismic mitigation, to appear in the *Proceedings of Structural Health Monitoring 2019*, I hereby agree to the following:

1. To grant to DEStech Publications, Inc., 439 North Duke Street, Lancaster, PA, 17602, copyright of the above named chapter/contribution (for U.S. Government employees to the extent transferable), in print, electronic, and online formats. However, the undersigned reserve the following:
 - a. All proprietary rights other than copyright, such as patent rights.
 - b. The right to use all or part of this article in future works.

DEStech Publications thereby retains full and exclusive right to publish, market, and sell this material in any and all editions, in the English language or otherwise.

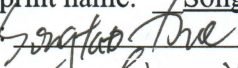
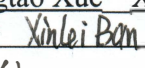
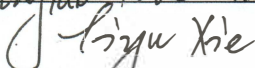
1 I warrant to DEStech Publications, Inc., that I am the (an) author of the above-named chapter/contribution and that I am the (a) copyright holder of the above-named chapter/contribution granted to DEStech Publications, Inc.

2 I warrant that, where necessary and required, I have obtained written permission for the use of any and all copyrighted materials used in the above-named chapter/contribution. I understand that I am responsible for all costs of gaining written permission for use of copyrighted materials.

3 I agree to assume full liability to DEStech Publications, Inc. and its licensee, and to hold DEStech Publications, Inc. harmless for any claim or suit filed against DEStech Publications, Inc. for violation of copyrighted material used in the above-named contribution.

Please sign and date this form and retain a copy for your records. Please include original form with your chapter/paper.

Thank you for your cooperation.

Please print name: Songtao Xue Xinlei Ban Liyu Xie
Signed:    Dated: 2019. 4. 25

439 NORTH DUKE STREET • LANCASTER, PENNSYLVANIA 17602-4967, U.S.A. Toll Free:
(866) 401-4337 • Tel: (717) 290-1660 • Fax: (717) 509-6100 E-mail: info@destechpub.com •
Internet address: www.destechpub.com